BCCIPβ modulates the ribosomal and extraribosomal function of S7 through a direct interaction

Qian Ba, Xiaoguang Li, Chao Huang, Junyang Li, Yijing Fu, Peizhan Chen, Juan Duan, Miao Hao, Yinghua Zhang, Jingquan Li, Chuanqi Sun, Hao Ying, Haiyun Song, Ruiwen Zhang, Zhiyuan Shen, and Hui Wang

Table of contents

Supplementary Methods

BCCIPβ-S7 interaction analysis by docking

The three-dimensional structures of BCCIPβ and S7 were predicted in a I-TASSER server according to the protein sequences without additional restraints [1]. The quality of models was estimated by the confidence score (*C*-score). Prior to the docking procedure, the coordinates of S7 and BCCIPβ models were subjected to energy minimization by CHARMm force field implemented in Discovery studio software. A ZDOCK server was utilized to perform unrestrained, pair wise, rigid body docking for BCCIPβ and S7, which could predict and evaluate the interactions in the BCCIPβ and S7 complex. Docking was accomplished without specifying the binding residues so that the results exhibited the most probable interaction patterns without any arbitrary restrains. From thousands of candidates, the ZDOCK server ranked the 50 most probable predictions on the basis of electrostatic complementarity, hydrophobicity, and geometry of the molecular surface. The important residues in the BCCIPβ-S7 complex were identified on the basis of docking *Z*-score.

Supplementary Results

The three-dimension structures of BCCIPα and BCCIPβ are different

Although BCCIPα and BCCIPβ share protein sequences with high similarity, their stereo structures are distinct. According to the simulation, the BCCIPα protein has a globular and compact structure. α-Helices and β-sheets are distributed in a staggered manner, making the structure more stable (Fig S2A). For BCCIPβ, the overall

structure resembles a rectangle with α-helices in the same direction, which gives it greater flexibility (Fig S2A). In regard to the N-terminal binding domain, the negative-charged groove in BCCIPβ is more open and larger than that in BCCIPα for S7 binding (Fig S2A). In addition, the presence of strong positive charges such as K235, K236, and K237 around the negatively charged pocket in BCCIPα (arrow in Fig S2A) may also prevent its association with S7. Therefore, the distinct three-dimension structures determine the differential capacity of BCCIPα and BCCIPβ to interact with S7.

Reference

1. Roy A, Kucukural A, Zhang Y. I-TASSER: a unified platform for automated protein structure and function prediction. *Nature protocols* **5**, 725-738 (2010).

Supplementary Figures

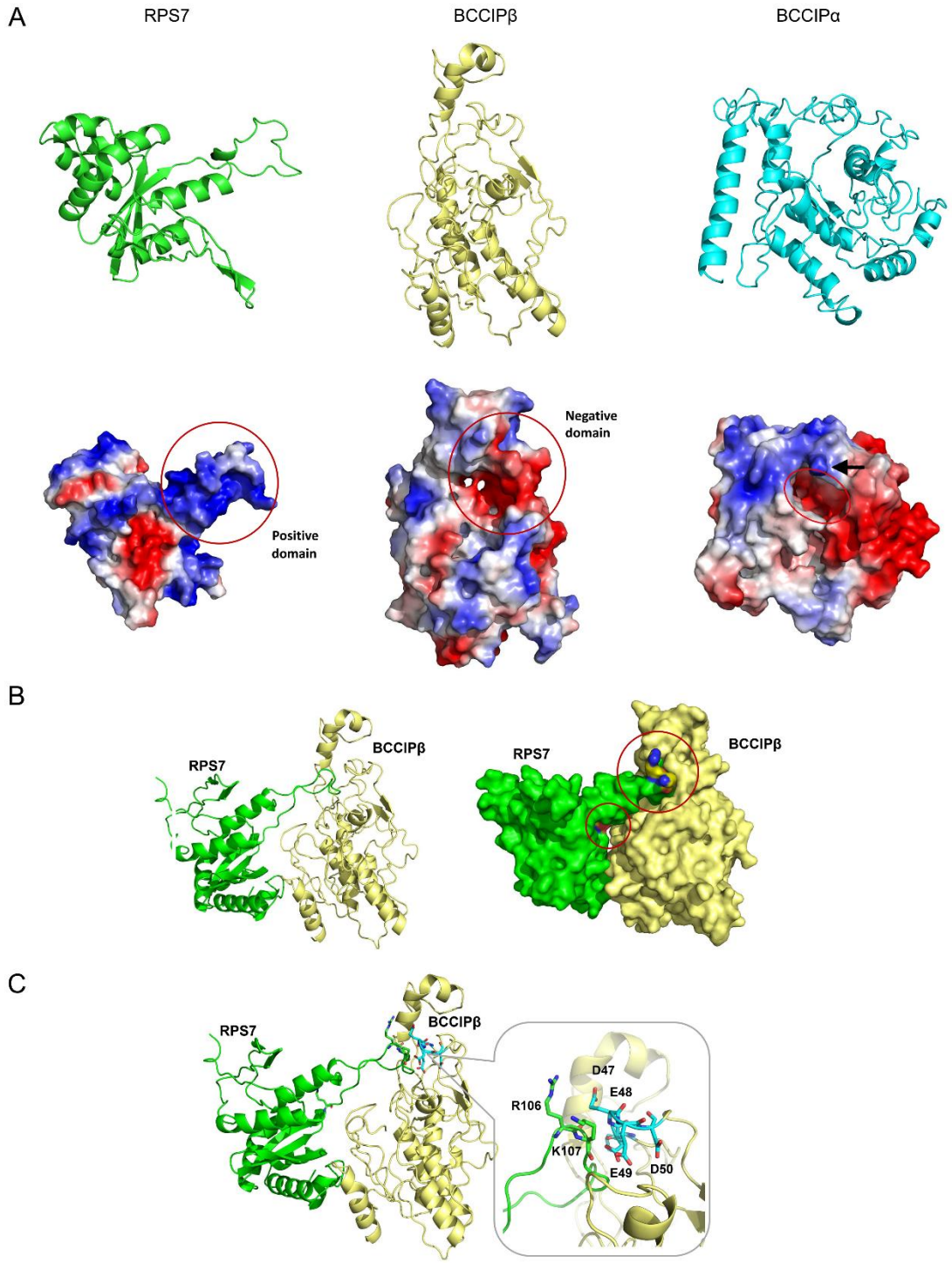

Supplementary Figure S1. (A) The predicted three-dimensional structures (upper panel) and the false red/blue charge-smoothed surfaces (lower panel) of S7, BCCIPβ, and BCCIPα are shown. Blue, positive charge; red, negative charge. The extension

arm with positive charge in S7 and the groove with negative charge in BCCIP β are indicated by circles. (B) The docking model of S7 and BCCIPβ. The positive area in S7 interacts with the negative area in BCCIPβ. (D) The predicted key amino acids for S7-BCCIPβ binding are shown.

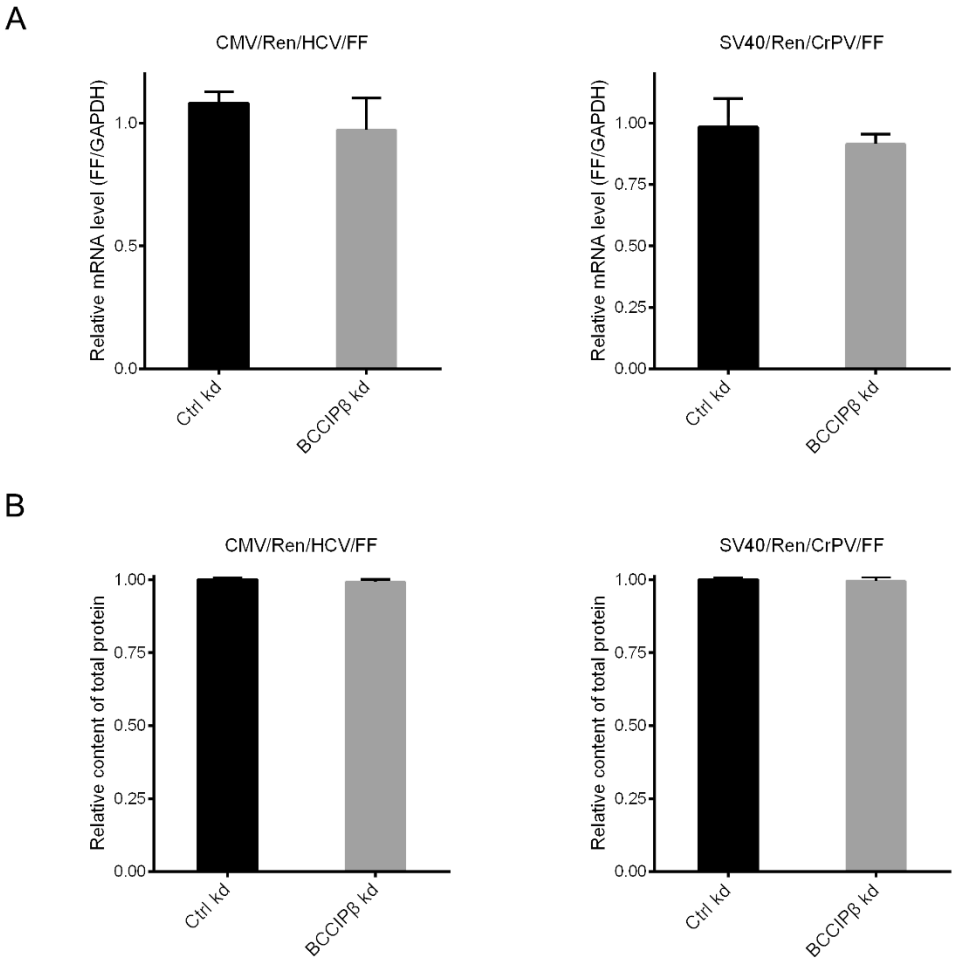

Supplementary Figure S2. (A) Control and BCCIPβ kd U2OS cells were transfected with the indicated bicistronic reporter plasmid, and mRNA levels of firefly luciferase (FF) were determined by realtime PCR. The primers were as follows: FF forward, 5'-CAT ACT CCA GGG TTA CGG-3', reverse, 5'-GGT ACT ATC GCA GCA TCT T-3'; and GAPDH forward, 5'-GGA GTC CAC TGG CGT CTT CAC-3', reverse, 5'-GAG GCA TTG CTG ATG ATC TTG AGG-3'. (B) Control and BCCIPβ kd U2OS cells were transfected with the indicated bicistronic reporter plasmid, and the total protein was harvested and measured.

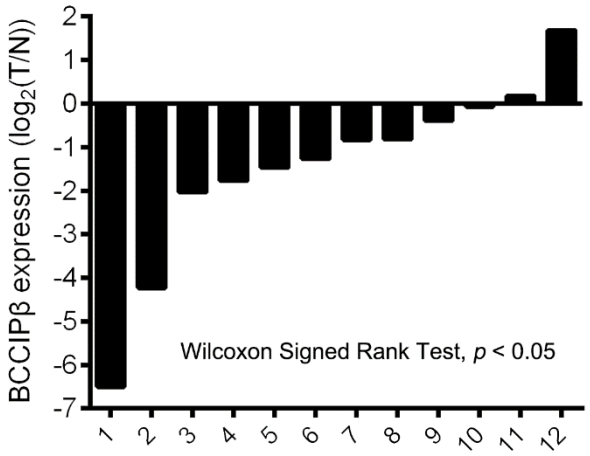

Supplementary Figure S3. BCCIPβ expression in 12 paired human liver cancer (T) and adjacent normal (N) tissues was determined by Western blotting. The protein level of BCCIPβ was quantitated by Image J and normalized to that of GAPDH.

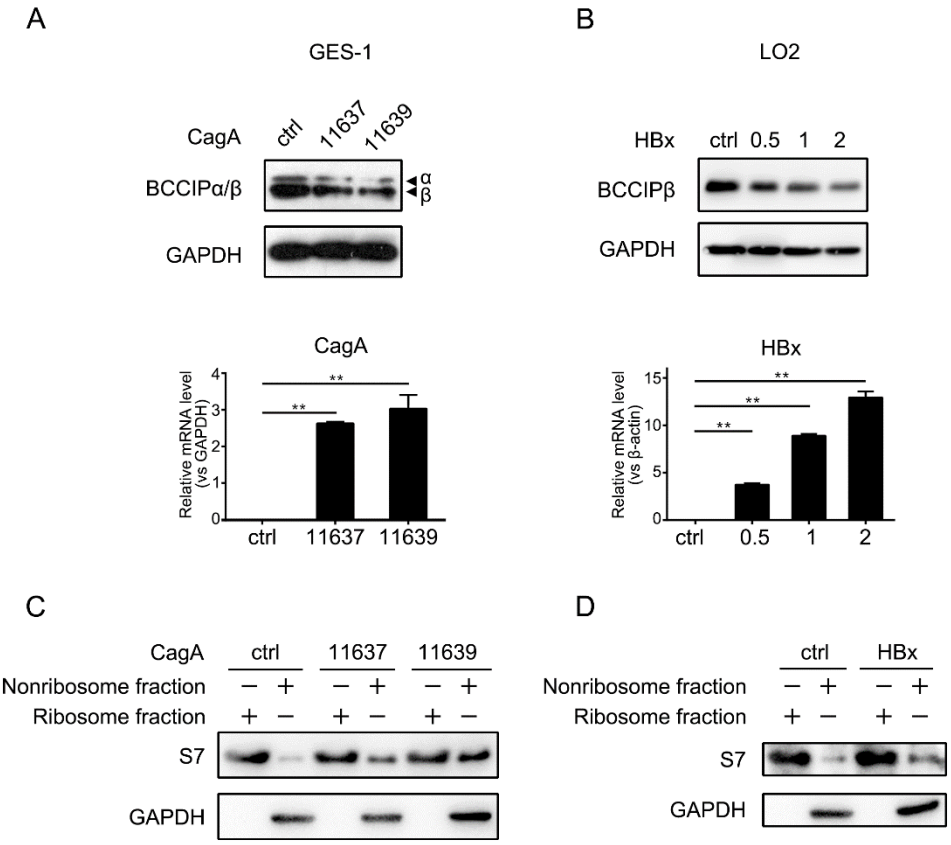

Supplementary Figure S4. CagA was ectopically expressed in the human gastric epithelial cell line, GES-1 (A), and HBx was ectopically expressed in human liver cells, LO-2 (B). Target proteins were detected by Western blotting (upper panel), and mRNA was determined by realtime PCR (lower panel). The primers were as follows: CagA 11637 forward, 5'-AAC AAC CAC AAA CCG AAG CG-3', reverse, 5'-ATC GTA TGA AGC GAC AGC GT-3'; CagA 11639 forward, 5'-CAG CAA GGT AAC GCA AGC AA-3', reverse, 5'- GCT TGC TCT ACC CCA CTG AA-3'; β-actin forward, 5'-GGC GGC ACC ACC ATG TAC CCT-3', reverse, 5'- AGG GGC CGG ACT CGT CAT ACT-3'; and GAPDH forward, 5'-GGA GTC CAC TGG CGT CTT CAC-3', reverse, 5'-GAG GCA TTG CTG ATG ATC TTG AGG-3'. (C and D) After transfection with CagA (C) or HBx (D) for 48 h, the proteins in nonribosomal and ribosomal fractions were separated and subjected to Western blotting.